Asian Journal of Chemistry; Vol. 32, No. 9 (2020), 2284-2292

ASIAN JOURNAL OF CHEMISTRY

https://doi.org/10.14233/ajchem.2020.22787

Controlled Synthesis, Characterization and Magnetic Properties of Unsymmetrical Heterodinuclear $Cu^{II}M^{II}$ (M = Co, Mn and Cd) Complexes in Alkoxo Bridged Acyclic Ligand Environment

DIPESH GHOSH

Department of Chemistry, Vivekananda Mission Mahavidyalaya, Chaitanyapur, Haldia-721645, India

Corresponding author: E-mail: dipesh105@hotmail.com

Received: 21 April 2020; *Accepted*: 9 June 2020; *Published online*: 20 August 2020; AJC-20027

This work reports the syntheses of heterodinuclear Cu(II)-Co(II), Cu(II)-Mn(II) and Cu(II)-Cd(II) complexes following a convenient single-pot synthetic procedure using the two asymmetric binucleating ligands. Site-specificity offered by one of the ligands' arms towards Cu(I) center has been successfully exploited here, avoiding all sorts of impending scrambling reactions. X-ray crystallography and ESI-mass spectral studies have been used to prove the exclusivity of these products. Magnetic studies at variable temperatures (4-300 K) have been proved inadequate to assign any spin-ground state for Cu(II)-Co(II) and Cu(II)-Mn(II) compounds.

Keywords: Heterodinuclear complexes, Crystal structure, ESR spectra, Magnetic studies.

INTRODUCTION

Studies on heterodinuclear metal complexes have received increasing attention in recent years because of their interesting physico-chemical properties arising from the presence of two dissimilar metal ions in close proximity [1-5]. Several binuclear active sites involving heterometal combinations, such as in bovine erythrocyte superoxide dismutase [Cu,Zn], purple acid phosphatase [Fe,Zn], human calcineurin [Fe,Zn], *etc*. are known to catalyze many exciting fundamental reactions of biological importance [6-9]. Individual metal ions of these combinations have inherent differences in their chemical behavior that appear to control the functioning of these enzymes under the constraints of protein microenvironment [10]. Asymmetry thus plays important role in biology [11-16].

Replication of such heterobimetallic analogs requires the development of unsymmetrical dinucleating ligands capable of incorporating dissimilar metal ions, in tandem [17,18]. This is always an arduous exercise because of the inherent difficulties in the preparation of such ligands involving multistep synthesis. Several phenol [19-24], alkoxo [25-29] and pyrazole [30,31] based asymmetric binucleating ligands have been successfully used in recent time to provide donor and coordination number asymmetry in some homodinuclear complexes. Syntheses of heterodinuclear complexes are however, possible under suitable experimental conditions, which allow the formation of mononuclear precursor complex to be used subsequently for heterocomplexation [32,33]. Such synthetic strategy has a general weakness of generating homodinuclear byproducts due to scrambling reactions. With the objective to avoid such unwanted reactions, a few binucleating asymmetric ligands have been reported recently involving chemically distinct donor set combinations with widely different affinities for the participating metal centers [3,4,31,34,35].

In this article, syntheses of heterodinuclear complexes of Cu(II)/Co(II), Cu(II)/Mn(II) and Cu(II)/Cd(II) combinations have been reported using the dinucleating asymmetric ligands, *viz*. methyl-2-{2-*bis*[(3,5-dimethylpyrazol-1-yl-methyl)amino]- 2-hydroxy propyl amino}cyclopent-1-ene-1-dithiocarboxylate (H_2L^2) and its pyrazolyl homologue (H_2L^3). X-ray crystallography, variable temperatures (300-3 K) magnetic measurements, ESI-mass spectrometry, electronic spectroscopy and EPR studies have been carried out to characterize these compounds.

EXPERIMENTAL

Magnetic moments of the powdered polycrystalline samples at room temperature were calculated from the data obtained on a PAR 155 vibrating sample magnetometer. Variable temper-

ature magnetic susceptibility data and magnetization measurements on powdered samples of complexes **1** and **3** were performed on a Cryogenic S600 SQUID magnetometer in the temperature range 3-400 K with an applied field of 0.1 T. A diamagnetic correction, estimated from Pascal's constants, was applied on the experimental susceptibilities to obtain molar paramagnetic susceptibilities. The EPR spectra of the samples were recorded on a Varian E-9 spectrometer working on X-band (9.25 GHz) which was equipped with an Oxford Instruments ESR9 helium flux cryostat at temperatures between 2 K and room temperature. Mass spectroscopy was performed on a LCQ Finnigan Electrospray Ionization Mass Spectrometer with electrospray ionization (ESI) source. All other measurements were done as described earlier [36].

Synthesis: The ligands H_2L^2 and H_2L^3 were prepared as described elsewhere. Solvents were reagent grade and dried from appropriate reagents [37] and distilled under nitrogen prior to use. All other chemicals were reagent grade, available commercially and used as received. **Caution!** Perchlorate salts of metal complexes are potentially explosive [38] and should be handled with great care.

Synthesis of $[CuCoL^3(\mu\text{-pz})]BPh_4\cdot CH_3CN$ (1): To a dry acetonitrile solution (50 mL) of H_2L^3 (0.2 g, 0.5 mmol) was added triethylamine (50 mg, 0.5 mmol) and then one equivalent of $Co(ClO_4)_2.6H_2O$ (0.18 g, 0.5 mmol) in solid while stirring under N_2. After 15 min, was added one equivalent amount of $[Cu(CH_3CN)_4]ClO_4$ (0.17 g, 0.5 mmol) in acetonitrile (10 mL), followed by pyrazole (35 mg, 0.5 mmol) and the resulting solution was stirred for *ca*. 10 min to get a red-brown solution. It was filtered and the filtrate volume was reduced to *ca*. 20 mL by rotary evaporation. Addition of $NaBPh_4$ (0.24 g) followed by cooling at 0 ºC afforded red-brown crystals. The compound was recrystallized from acetonitrile. Yield: 90 mg (19%). Elemental analysis calcd. (found) % for $C_{47}H_{50}N_9S_2OCuCoB$: C, 59.17 (59.41); H, 5.24 (5.54); N, 13.22 (13.11). IR (KBr, ν_{max}, cm^{-1}): 1581 s (C–C) + (C–N)/pyrazole ring, 1461 s, 1424 m (C–C + C–N), 735, 705 s (BPh_4^-). μ_{eff}: 4.5 μ_B at 25 ºC.

Synthesis of $[CuCoL^m(\mu\text{-pz})]BPh_4\cdot CH_3CN$ (2)*: This complex was synthesized following a procedure essentially identical to that described for complex **1**, using H_2L^2 as the asymmetric ligand. Yield: 115 mg (23%). Elemental analysis calcd. (found) % for $C_{49}H_{54}N_9S_2OCuCoB$: C, 59.93 (60.7); H, 5.50 (5.34); N, 12.84 (12.53). IR (KBr, ν_{max}, cm^{-1}): 1584 m (C–C), 1552 m (C–N)/pyrazole ring, 1472 s, 1421 m (C–C + C–N), 734 & 705 s (BPh_4^-). MS: *m/z* 663.4 $[M\text{-}BPh_4]^+$. μ_{eff}: 4.56 μ_B at 25 ºC. (*L^m stands for modified ligand framework)

Synthesis of $[CuMnL^m(\mu\text{-pz})]BPh_4$ (3): Acetonitrile solution of Et_3N (50 mg, 0.5 mmol), $Mn(ClO_4)_2\cdot 6H_2O$ (0.18 g, 0.5 mmol), $[Cu(CH_3CN)]ClO_4$ (0.17 g, 0.5 mmol in 10 mL of acetonitrile) and dimethyl pyrazole (0.05 g, 0.5 mmol) were added sequentially to a solution of H_2L^3 (0.2 g, 0.5 mmol) in CH_3CN (30 mL) at room temperature under nitrogen atmosphere and stirred for *ca*. 15 min. The resulting brown solution was then exposed to air and the stirring was continued further for 2 h. The deep brown solution thus obtained was filtered off, combined with $NaBPh_4$ (0.17 g) and then cooled to 0 ºC to get brown microcrystalline solids. The product was recrystallized from acetonitrile. Yield: 86 mg (18%). Elemental analysis calcd. (found) % for $C_{47}H_{51}N_8S_2OCuMnB$: C, 60.24 (60.81); H, 5.45 (4.93); N, 11.96 (12.11). IR (KBr, ν_{max}, cm^{-1}): 1580 s (C–C), 1550 m (C–N)/pyrazole ring, 1470 s, 1425 m (C–C + C–N), 738 & 707 s (BPh_4^-). μ_{eff}: 3.92 μ_B at 25 ºC.

Synthesis of $[CuMnL^3(\mu\text{-pz})]BPh_4$ (4): This complex was synthesized following an identical procedure as mentioned above for complex **3** using pyrazole as the bridging ligand instead of dimethylpyrazole. Yield: 60 mg (13%). Elemental analysis calcd. (found) % for $C_{45}H_{47}N_8S_2OCuMnB$: C, 59.46 (59.29); H, 5.17 (4.74); N, 12.33 (13.41). IR (KBr, ν_{max}, cm^{-1}): 1581 s (C–C) + (C–N)/pyrazole ring, 1461 s, 1425 m (C–C + C–N); 736 & 707 s (BPh_4^-). MS: *m/z* 589.1 $[M\text{-}BPh_4]^+$. μ_{eff}: 3.91 μ_B at 25 °C.

Synthesis of $[CuCdL^2(\mu\text{-pz})(CH_3CN)]BPh_4\cdot 0.25CH_3CN$ (5): Et_3N (50 mg, 0.5 mmol), $Cd(OAc)_2\cdot 2H_2O$ (133 mg, 0.5 mmol), $[Cu(CH_3CN)_4]ClO_4$ (0.17 g, 0.5 mmol in 10 mL CH_3CN) and pyrazole (35 mg, 0.5 mmol) were added in sequence to a solution of H_2L^2 (0.23 g, 0.5 mmol) in dry CH_3CN (50 mL) under nitrogen. The solution was stirred for 10 min. The resulting red-brown solution was exposed to atmospheric oxygen and stirred further for *ca*. 2 h. The colour of the solution became deep brown at this stage. The solution was filtered, the filtrate volume, after adding $NaBPh_4$ (0.17 g), was reduce to *ca*. 10 mL by rotary evaporation. Dark microcrystalline compound obtained at this stage after cooling at 0 ºC was collected by filtration, washed with diethylether, dried in vacuo and finally recrystallized from CH_3CN. Yield: 85 mg (16%). Elemental analysis calcd. (found) % for $C_{51.5}H_{58.75}N_{9.25}S_2OCuCdB$: C, 57.53 (57.52); H, 5.47 (5.35); N, 12.05 (12.17). IR (KBr, ν_{max}, cm^{-1}): 1578 m (C–C), 1558 m (C–N)/pyrazole ring, 1473 s & 1423 m (C–C + C–N), 737 & 708 s (BPh_4^-). μ_{eff}: 1.72 μ_B at 25 ºC.

X-ray crystallography: Intensity data for complex **1** were measured at 173 K on a Rigaku AFC7R diffractometer with Mo*K*α radiation and the ω:2θ scan technique such that θ_{max} was 27.5º. Intensity data for complexes **3** and **5** were measured at 223 K on a Bruker AXS SMART CCD diffractometer fitted with Mo*K*α radiation using ω scans such that θ_{max} was 30.1 and 30.0º, respectively. Data were corrected for Lorentz and polarization effects as well as for absorption employing empirical procedures (for complex **1** [39] and for complexes **3** & **5** [40]). The structures were solved by heavy-atom methods [41] and refined (anisotropic displacement parameters, H atoms in the riding model approximation and a weighting scheme of the form $w = 1/[\sigma^2(F_o^2) + aP^2 + bP]$ where $P = (F_o^2 + 2F_c^2)/3$) by a full-matrix least-squares procedure based on F^2 [42]. Residual electron density peaks consistent with the presence of solvent molecules of crystallization were noted in the refinement of complex **5**. These were modeled as a partially occupied (25%, isotropic displacement parameters and no H atoms) acetonitrile molecule disordered about a center of inversion. The rather large residual electron density peaks in complexes **3** and **5** are located in the vicinity of Mn and Cd centers, respectively. Crystal data and refinement details are collated in Table-1. Molecular structures were drawn with 50% displacement ellipsoids using the ORTEP program [43]. Calculations were performed employing the teXsan package [44].

TABLE-1
CRYSTAL DATA FOR COMPLEXES **1**, **3** AND **5**

	Complex **1**	Complex **3**	Complex **5**
Composition	$C_{47}H_{50}N_9OBCoCuS_2$	$C_{47}H_{51}N_8OBCuMnS_2$	$C_{51.5}H_{58.75}N_{9.25}OBCdCuS_2$
Formula weight	954.4	937.4	1074.2
Crystal system	Monoclinic	Monoclinic	Monoclinic
Space-group	$P2_1/c$	$P2_1/c$	$P2_1/n$
Crystal size (mm^{-3})	0.16 × 0.27 × 0.32	0.10 × 0.26 × 0.42	0.05 × 0.31 × 0.31
Colour	Red	Dark-red	Red-brown
a (Å)	12.476(2)	13.5180(11)	13.1572(4)
b (Å)	20.471(3)	9.6225(8)	19.3865(6)
c (Å)	18.085(5)	33.815(3)	19.8057(7)
α (°)	90	90	90
β (°)	99.14(2)	94.833(2)	90.163(1)
γ (°)	90	90	90
V ($Å^3$)	4560(1)	4383.0(6)	5051.9(3)
Z	4	4	4
$d_{calc.}$ ($g\ cm^{-3}$)	1.390	1.421	1.412
Temp. (K)	173	223	223
λ (Å)	0.71073	0.71073	0.71073
μ (cm^{-3})	9.69	9.16	9.72
No. data ($I \geq 2\sigma(I)$)	6090	9130	8212
No. of variables	560	552	612
R^a	0.042	0.069	0.074
$R_w{}^b$	0.110	0.212	0.218

$^aR = \Sigma||F_o| - |F_c||/\Sigma|F_o|$. $^bR_w = [\Sigma w(|F_o| - |F_c|)^2/\Sigma w|F_o|^2]^{½}$.

RESULTS AND DISCUSSION

Heterodinuclear complexes *viz*. Cu(II)-Co(II) (**1**, **2**), Cu(II)-Mn(II) (**3**, **4**) and Cu(II)-Cd(II) (**5**) were conveniently synthesized as exclusive products by single-pot synthesis using the alcohol-based binucleating "end-off" ligands [45] H_2L^2 and H_2L^3. The site specificity of Cu(I) ion for the bidentate NS donor arm of these ligands has been exploited here to achieve the objective. The precursor cuprous complexes which are susceptible to aerial oxidation, give the desired products when exposed to atmospheric oxygen. The exclusivity of the products obtained from these reactions, has been confirmed by X-ray crystal structure analyses of complexes **1**, **3** and **5** and ESI-mass spectral analyses of complexes **2** and **4**. The structures reveal a combination of donor and coordination number asymmetry in these molecules [46].

Fig. 1a and b shows a parent ion peak at around *m/z* = 663, corresponding to the ionic entity $[M\text{-}BPh_4]^+$ while the parent ion peak at around *m/z* = 589 for complex **4**, indicate the exclusive presence of hetertodinuclear species in the bulk sample of this complex. The data clearly indicate the site specificity offered by these ligands. No ion peak due to homodinuclear species is detected in these compounds. There are only a few reports [45,47-50] of similar heterodinuclear complexes in acyclic ligand environments, most of which [47-50] were prepared with a bit of luck using symmetric binucleating ligands.

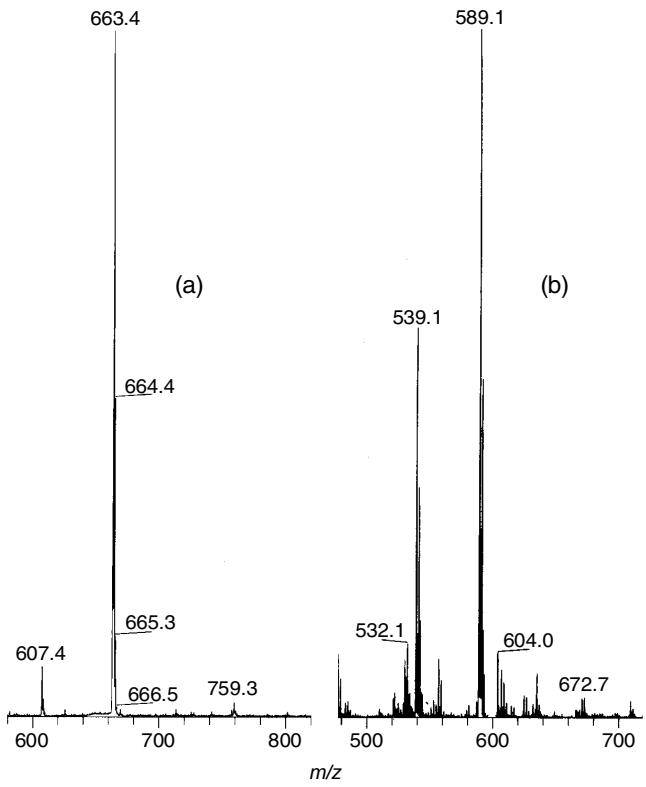

Fig. 1. ESI-MS in acetonitrile of (a) **2** and (b) **4**

The coordination ability of H_2L ligands is of particular interest here. The two dimethyl pyrazolyl arms of H_2L^2 which form the tridentate pocket, remain intact only in complex **5** when the larger Cd^{2+} ion is housed in that site. As shown in **Scheme-I**, one of the dimethyl pyrazolyl arms in this ligand, has undergone an exchange reaction with extraneous pyrazole, added as bridge between the metal centers during the formation of complex **2** (confirmed by mass spectrometry, Fig. 1a). When dimethyl pyrazole is added as a bridging ligand in the synthesis of complex **3**, it is exchanged with one of the pyrazolyl arms

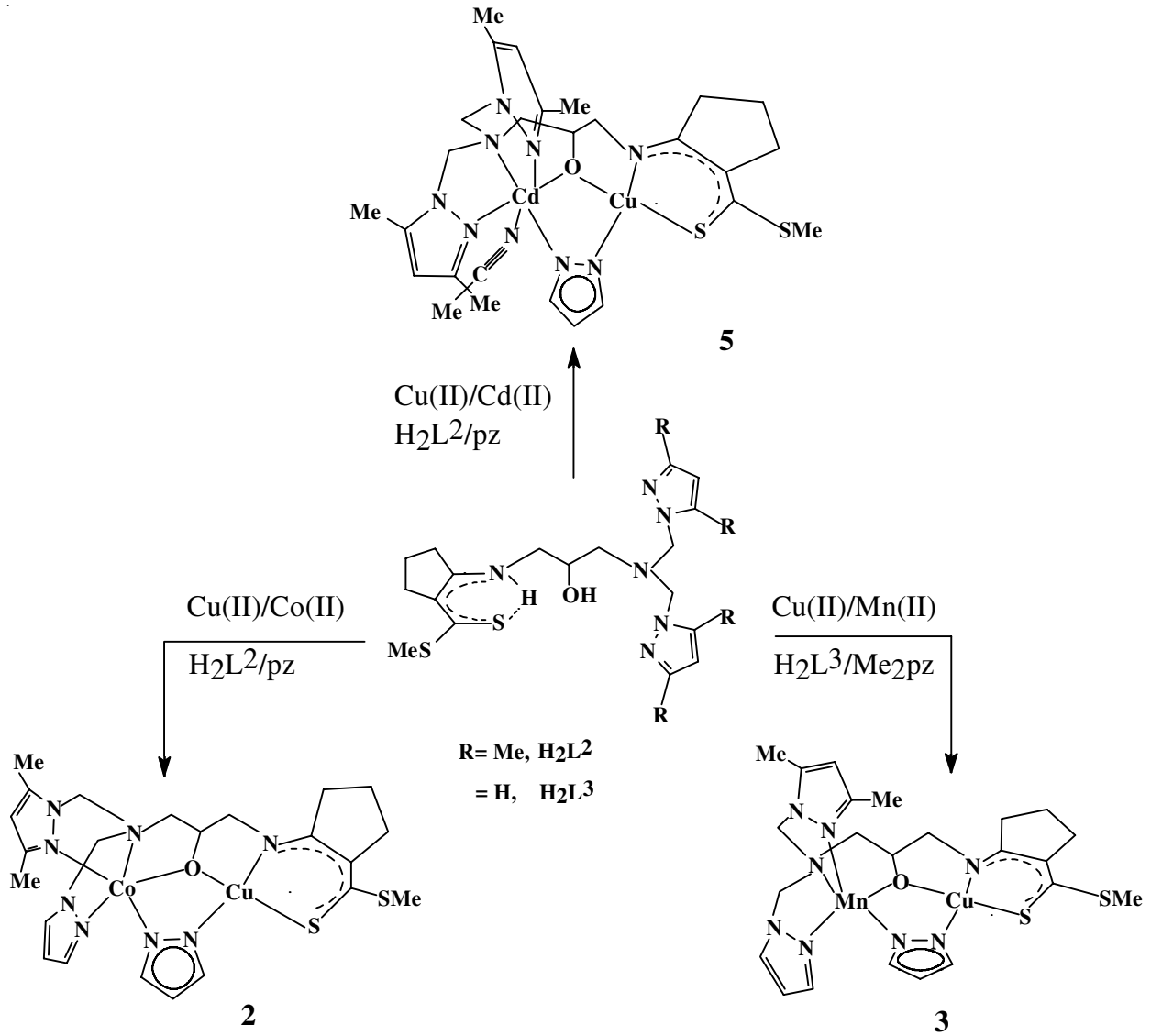

Scheme-I

of H_2L^3 and the released pyrazole molecule is accommodated to bridge the metal centers as confirmed by X-ray crystallographic analysis. These two contrariant ways of ligand exchange lead to the generation of a new coordinated ligand $(L^m)^{2-}$ with assorted donor arms. The steric constraints due to smaller sizes of Co(II) and Mn(II) compared to cadmium(II), probably force the ligand molecules (both H_2L^2 and H_2L^3) to rearrange by exchange reaction. This as well as the high solubilities of the reported compounds, requiring tetraphenyl borate for crystallization, could be the reasons for their reported low yields (< 20%).

Description of crystal structures: The molecular structures of the cations in complexes **1**, **3** and **5** are shown in Figs. 2-4, respectively and selected geometric data are listed in Table-2. Complex **1** crystallizes with a molecule of acetonitrile solvent but this does not form any significant intermolecular interaction. Complex **5** also crystallizes with a acetonitrile molecule coordinated to the cadmium atom and a partially occupied and disordered non-interacting acetonitrile molecule. The Cu is bound to the bidentate arm and the M (for complex **1**, M = Co; complex **3**, M = Mn and complex **5**, M = Cd) is bound to the tridentate arm. The metal ions are bridged by the alkoxide O1 oxygen of the asymmetric ligands and the pyrazolate nitrogens of the

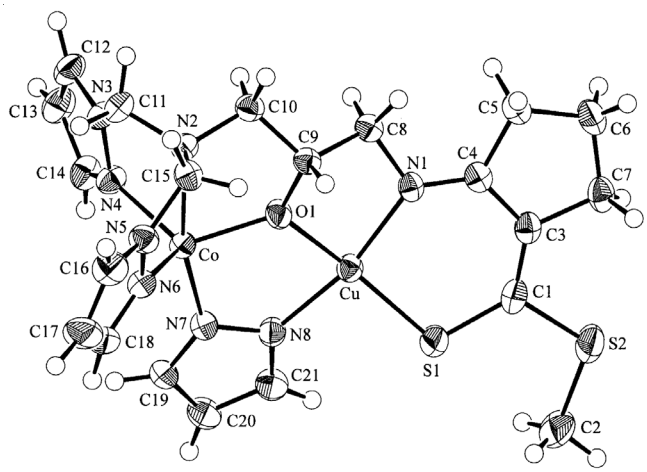

Fig. 2. An ORTEP view of **1** with the atom numbering scheme

TABLE-2
SELECTED BOND LENGTHS (Å) AND ANGLES (°) FOR **1**, **3** AND **5**

Bond lengths (Å)				Bond angles (°)			
	1	**3**	**5***		**1**	**3**	**5***
	M = Co	M = Mn	M = Cd		M = Co	M = Mn	M = Cd
Cu···M	3.38	3.39	3.60	S(1)-Cu-O(1)	170.10(7)	177.77(11)	178.31(12)
Cu-S(1)	2.2178(11)	2.2191(11)	2.2239(15)	S(1)-Cu-N(1)	97.25(8)	97.74(10)	96.99(13)
Cu-O(1)	1.914(2)	1.894(3)	1.905(3)	S(1)-Cu-N(8)	93.36(8)	93.70(10)	89.70(13)
Cu-N(1)	1.959(2)	1.942(3)	1.963(4)	O(1)-Cu-N(1)	84.12(9)	83.92(13)	84.27(15)
Cu-N(8)	1.991(3)	1.993(4)	1.993(4)	O(1)-Cu-N(8)	87.01(9)	84.66(13)	89.13(15)
M-O(1)	1.912(2)	1.892(3)	2.210(3)	N(1)-Cu-N(8)	165.95(11)	168.52(14)	171.91(18)
M-N(2)	2.293(3)	2.102(3)	2.551(4)	O(1)-M-N(2)	78.97(9)	82.86(2)	71.49(11)
M-N(4)	2.024(3)	2.166(3)	2.235(4)	O(1)-M-N(4)	113.25(10)	117.44(15)	109.77(13)
M-N(6)	2.010(3)	2.049(3)	2.243(4)	O(1)-M-N(6)	124.70(10)	135.14(16)	98.20(14)
M-N(7)	2.014(3)	1.940(3)	2.167(4)	O(1)-M-N(7)	87.71(10)	86.71(13)	80.91(14)
S1-C(1)	1.727(3)	1.715(4)	1.680(6)	N(2)-M-N(4)	77.80(10)	81.01(12)	71.02(13)
				N(2)-M-N(6)	77.79(10)	80.28(13)	71.53(12)
				N(2)-M-N(7)	166.67(9)	169.16(13)	152.39(14)
				N(4)-M-N(6)	109.70(11)	100.52(13)	121.95(15)
				N(4)-M-N(7)	107.49(11)	106.58(14)	121.16(16)
				N(6)-M-N(7)	110.81(11)	105.35(15)	112.61(15)
				Cu-O(1)-M	124.16(11)	126.77(15)	121.98(16)

*Cd-N(9), 2.622(5); O(1)-Cd-N(9), 165.43(15); N(2)-Cd-N(9), 119.49(15); N(4)-Cd-N(9), 83.81(17); N(6)-Cd-N(9), 77.98(16) and N(7)-Cd-N(9), 87.57(17)'

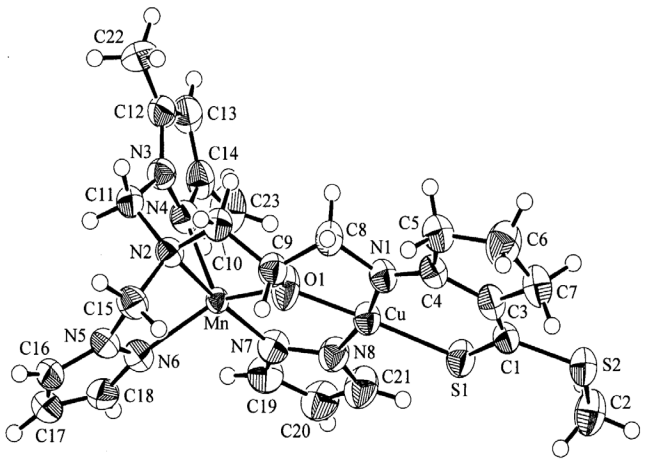

Fig. 3. An ORTEP view of complex **3** with the atom numbering scheme

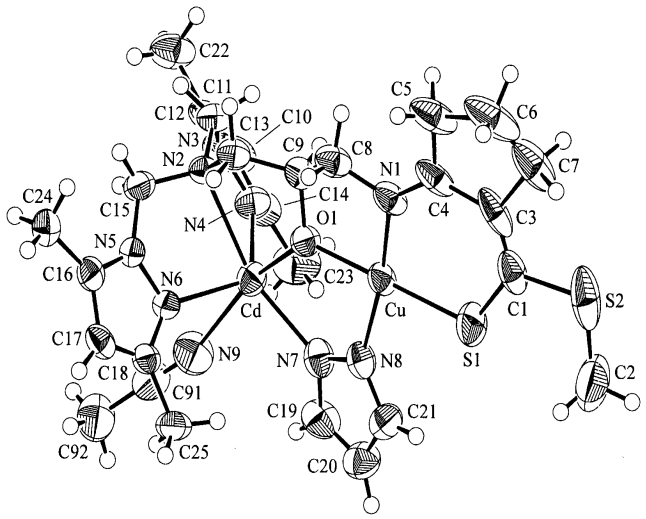

Fig. 4. Molecular structure of **5** showing the atom numbering (50% probability ellipsoids)

extraneous ligand. The Cu centers exist in distorted square planar geometries with O(1), N(1) and S(1) of the asymmetric ligands and one nitrogen N(8) from the bridging pyrazolate. The Cu atom lies 0.07, 0.01 and 0.03 Å, out of the least-squares plane in complexes **1**, **3** and **5**, respectively. The geometry of M center in complexes **1** and **3** are better described as a square based pyramidal distorted trigonal bipyramidal (SBPDTB) [51,52]. The discriminating parameter τ [53] between a square pyramid (τ = 0) and a trigonal bipyramid (τ = 1) is 0.7 for complex **1** and 0.57 for complex **3**. In this description, O(1), N(4) and N(6) atoms of the asymmetric ligands form the trigonal base and the the remaining N(2) together with the pyrazolate N(7) atom define the axial positions. The Co and Mn atoms are displaced by about 0.40 and 0.30 Å, respectively from the trigonal plane toward the axial N(7) atom. The axial M-N distances in complex **1** are longer than those of complex **3**: Co-N(2), 2.293(3) (Mn-N(2), 2.102(3) Å); Co-N(7), 2.014(3) (1.940(3) Å). As a consequence, the equatorial bonds are shortened in complex **1** with respect to those of complex **3**: Co-N(4), 2.024 (3) (2.166(3) Å); Co-N(6), 2.010(3) (2.049(3) Å). Co-O(1) (1.912(2) Å) and Mn-O(1) (1.892(3) Å) distances are similar. In terms of bond angles, the greatest difference is found in the O(1)-M-N(6) angle which is 124.70(10) for M = Co compared with 135.14(16) for M = Mn.

The situation for cadmium center in the structure of complex **5** is somewhat different from those operating in the cations of complexes **1** and **3** owing to the incorporation of an acetonitrile molecule in its coordination sphere. A N5O donor set defines the coordination environment around the Cd atom. The Cd-N(9) distance of 2.622(5) Å is the largest among the Cd-N distances (Table-2). The coordination geometry about Cd may be described as distorted octahedral but the greatest deviation from the ideal geometry is reflected in the N(4)-Cd-N(6) angle of 121.95(15) instead of 180 . An alternative description is one based on a trigonal prism where two trigonal faces

are defined by O(1), N(2) and N(6) and N(4), N(7) and N(9) atoms. In this description, Cd lies 1.45 Å below the first face and 1.05 Å above the second. Clearly, neither description is appropriate and so the coordination geometry may be described as somewhat intermediate between these two extremes. The bridge angle Cu-O(1)-M are 124.16(11), 126.77(15) and 121.98 (16) in complexes **1**, **3** and **5**, respectively. The S(1)-C(1) distances (1.680(6)-1.727(3) Å) indicate thiolate character of the sulfur, a feature already noted for 2-aminocyclopentene based dithiocarboxylate moiety [54,55].

The Cu···M separations are 3.38, 3.39 and 3.60 Å in the complexes **1**, **3** and **5**, respectively.

Magnetic properties: Magnetic measurements of representative CuM complexes (**1** and **3**) have been carried out in the temperature range 2-300 K. The $\chi_M T$ *vs.* T curve for the CuCo dimer **1** shows a gradual decrease of the $\chi_M T$ product from about 0.7 emu K mol^{-1} to a plateau value of about 0.3 emu.K.mol^{-1} at 50 K, followed by a steeper decrease towards zero for lower temperature (Fig. 5). It is difficult to predict what the high temperature (spin-only) value for a five coordinated Co(II) ion should be. Six coordinated high-spin Co(II) complexes in octahedral surroundings typically have spin-only $\chi_M T$ values of about 2.8 to 3.8 emu K mol^{-1}. Those of tetrahedrally surrounded Co(II) ions are generally lower at around 2.8 emu K mol^{-1}. It is clear that these literature values are far from the observed value of 0.7 emu K mol^{-1}. It is possible that Co(II) ion is in the low-spin configuration. In that case the $\chi_M T$ product is expected to be around 0.6 to 0.9 emu K mol^{-1}. Even in that case the spin-only value would be above 1.0 emu K mol^{-1}, (assuming 0.4 emu K mol^{-1} for copper ion). The fact that the $\chi_M T$ product decreases on lowering the temperature suggests antiferromagnetic exchange coupling between the two metal ions. The low-temperature $\chi_M T$ value of 0.3 emu K mol^{-1} is less than expected for any spin state higher than S = 0 (assuming g > 2). The same feature is shown by the magnetization curve recorded for fields up to 6.5 T at 2 K. The maximum magnetization value found is 1800 emu/mol, or about 0.32 μ_B, again less than expected even for S = 1/2 (0.5 μ_B at g = 2). Therefore it is hardly possible to obtain any definite information on the magnitude of antiferromagnetic exchange coupling and the nature of the spin ground state. The magnetic measurements were repeated on a new sample but gave exactly the same results.

The magnetic susceptibility curve of Cu(II)-Mn(II) heterodimer **3** looks similar to that of complex **1** (Fig. 6). Thus, at high temperatures, the $\chi_M T$ product is about 1.2 emu K mol^{-1}, decreasing with lowering the temperature to about 0.5 emu K

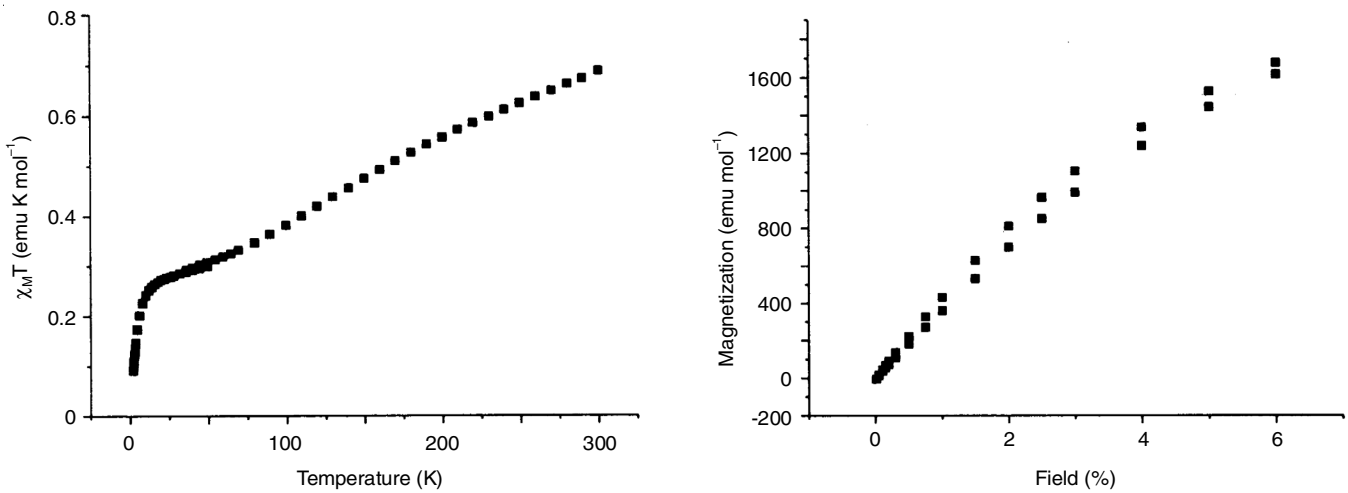

Fig. 5. $\chi_M T$ *vs.* T and magnetization *vs.* field plots for the Cu(II)-Co(II) heterodimer **1**

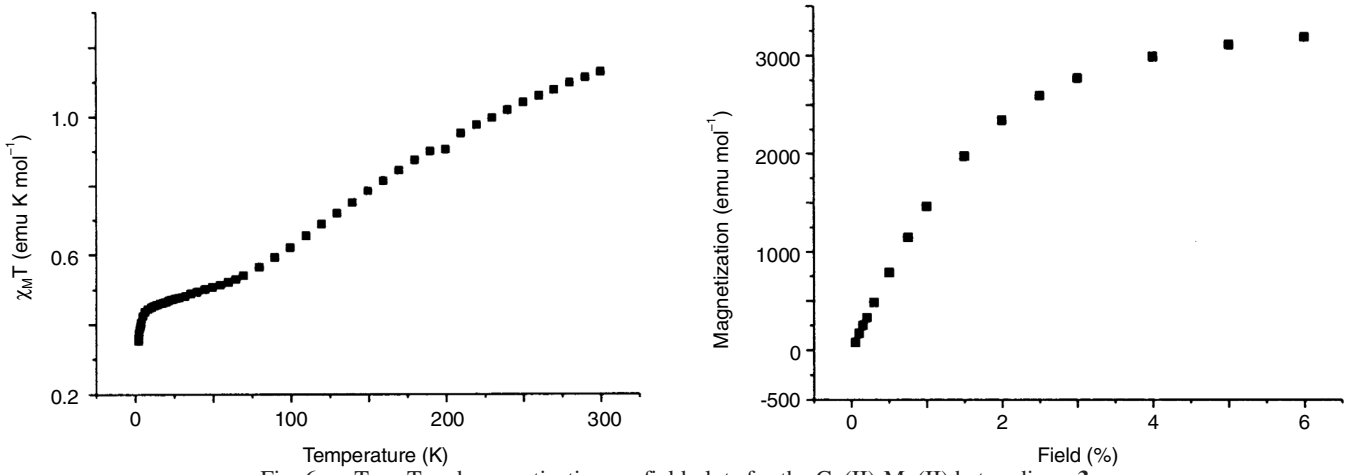

Fig. 6. $\chi_M T$ *vs.* T and magnetization *vs.* field plots for the Cu(II)-Mn(II) heterodimer **3**

mol^{-1} at 10-50 K, before going towards zero at very low temperatures. Manganese in the +2 oxidation state (high-spin) generally has spin 5/2 and isotropic g values of about 2. Copper(II) generally has g values of about 2.1-2.3 and spin 1/2. Hence, the spin-only $\chi_M T$ value for this complex is expected to be in the region of 4.8 emu K mol^{-1}.

Obviously, the non-zero slope of $\chi_M T$ *vs.* T curve at 300 K, indicates that some effect of exchange interaction on the $\chi_M T$ value is to be expected even at this temperature. However, the low-temperature plateau value of about 0.5 emu K mol^{-1} is reminiscent of an S = 1/2 ground state with a g value of about 2.3. With the present combination of ions, such a spin ground state is impossible to obtain. Although not common, it is possible to have Mn(II) in the low-spin state. In such case, the spin of the ion would be S = 1/2 and the g values should become anisotropic. Even in that case the spin ground state would be S = 0 or S = 1 depending on the type of exchange interaction. The magnetization curve saturates at about 3200 emu/mol or 0.58 μ_B, which does not correspond to any possible spin state. Hence, also in this case the results are inconclusive. The room temperature magnetic moment of the Cu(II)-Cd(II) complex **5** is 1.72 μ_B, as expected for a simple S = ½ paramagnet.

EPR studies: The X-band of EPR spectrum of Cu(II)-Cd(II) complex **5**, recorded at ambient temperature (CH_3CN/toluene, 1:3 v/v) is displayed in Fig. 7. The overall features are almost identical to those of the Cu(II)-Zn(II) compounds published earlier [56], involving a four line pattern, typical of a mononuclear Cu(II) center ($^{63,65}Cu$, $I = {}^3/_2$) with <g> = 2.09. Each of the stronger lines is split into three components due to nitrogen super-hyperfine couplings (^{14}N, $I = 1$) with $A_N = 15.6 \times 10^{-4}$ cm^{-1}, indicating strong Cu-N interactions from the bridging pyrazolyl nitrogen.

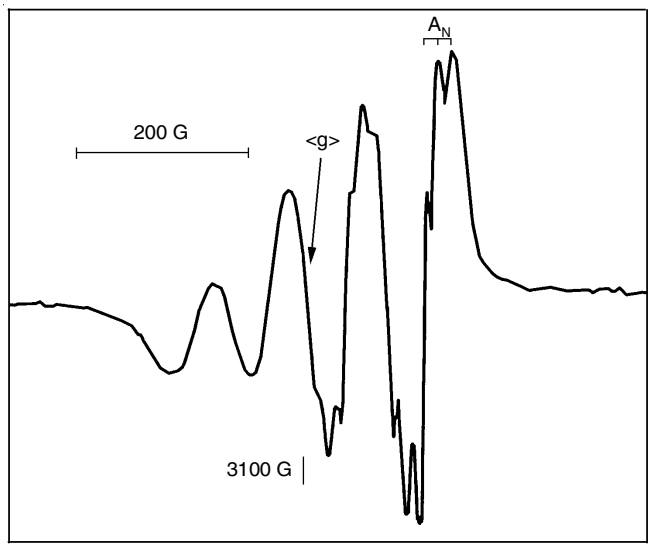

Fig. 7. EPR spectrum of **5** in CH_3CN/toluene (1:3 v/v) solution at room temperature

Electronic studies: Table-3 summarizes the electronic spectral data for the complexes **1-5**, recorded in acetonitrile solution. Three representative spectra (complexes **2**, **4** and **5**) are displayed in Fig. 8. Spectral features are grossly identical in the visible region, each involving two low-intensity bands in the 705-682 nm (ε, 295-87 mol^{-1} cm^2) and 531-508 nm (ε, 520-300 mol^{-1} cm^2) regions, arising from ligand-field transitions. For complex **5**, these can be safely assigned as originating from $d_{z^2} \rightarrow d_{x^2-y^2}$ and d_{xz}, $d_{yz} \rightarrow d_{x^2-y^2}$ transitions, respectively, as expected for a square planar Cu(II) center [57,58]. In remaining complexes **1-4**, the metal ions in the adjacent ligand compartment will also contribute in the visible region of the spectra as judged from their increased intensity (Table-3). For example, pentacoordinated Co(II) centers in complexes **1** and **2** are expected to show up two ligand-field bands close to the above regions [36,59,60]. The observed features are thus arising from a combination of the ligand-field contributions of the participating metal centers.

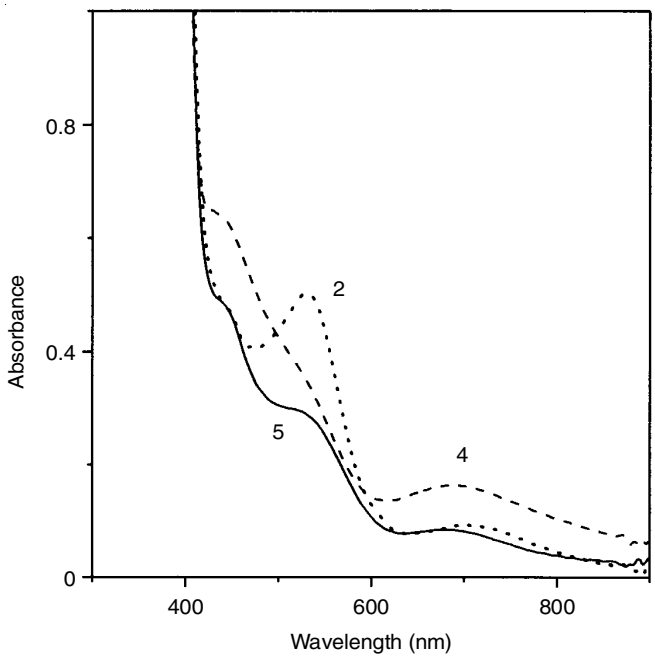

Fig. 8. Absorption spectra of complexes **2** (····), **4** (----) and **5** (—) in CH_3CN

In addition, the spectra also contain two strong bands in the near-UV region, both having charge-transfer origin [56]. The one at 443-428 nm region, appears mostly in the form of

TABLE-3
ELECTRONIC SPECTRAL DATA FOR THE COMPLEXES **1-5** IN CH_3CN

Complex	λ_{max}/nm (ε, mol^{-1} cm^2)
1	702 (120), 525 (520), 443 (sh), 383 (14400), 331 (17600), 289 (17900), 275 (15000)
2	705 (87), 531 (470), 442 (sh), 383 (14000), 330 (17000), 288 (18050), 274 (15800)
3	689 (235), 508 (sh), 428 (1100), 383 (8350), 330 (11980), 288 (10900)
4	690 (295), 519 (sh), 431 (1170), 381 (11800), 330 (16700), 288 (14800)
5	682 (89), 521 (300), 438 (sh), 383 (10400), 328 (15250), 288 (12900), 275 (11500)

shoulder, is due to N/pyrazolyl → Cu(II) charge-transfer while the other at 383 nm (ε, 14400-8350 mol^{-1} cm^2) is due to S(π) → Cu(II) charge-transfer [61]. The remaining bands in the UV region are due to ligand-localized transitions.

Conclusion

This article reports the syntheses and characterization of heterodinuclear Cu(II)-Co(II), Cu(II)-Mn(II) and Cu(II)-Cd(II) complexes (**1-5**) obtained by a convenient single-pot synthetic procedure. Site-specificity offered by the bidentate NS donor arms of the asymmetric ligands H_2L^2 and H_2L^3 towards the soft Cu(I) center, has been successfully exploited here to get the desired heterodinuclear products, avoiding all sorts of impending scrambling reactions that may lead to homodinuclear side products. The exclusivity of the products has been confirmed by X-ray crystallographic and ESI mass spectral analysis. Cu(II)-Co(II) and Cu(II)-Mn(II) complexes show antiferromagnetic interactions as revealed from variable temperature (2-300 K) magnetic measurements. The results ($\chi_M T$ *vs*. T plots) follow the observed trends, reported earlier for macrocyclic heterodinuclear complexes with similar metal ion combinations [62]. Strong metal-pyrazolyl nitrogen interactions as revealed from the EPR spectrum of Cu(II)-Cd(II) complex **5** probably generate the required pathway for these antiferromagnetic interactions for which, unfortunately, we are unable to assign any spin ground state.

ACKNOWLEDGEMENTS

The author thanks to ERO(UGC), Kolkata for financial support under MRP No. F. PSW-233/15-16(ERO) dated 21.11. 2016. Magnetic studies done by Prof. A. Caneschi, Università degli Studi di Firenze, Firenze, Italy gratefully acknowledged, Thanks are also due to Prof. M. Chaudhury, IACS, Kolkata for his continuous support; Prof. E.R.T. Tiekink, Sunway University, Malaysia and Dr. M. Maity, Behala College, Kolkata, India for single crystal X-ray diffraction study.

CONFLICT OF INTEREST

The authors declare that there is no conflict of interests regarding the publication of this article.

REFERENCES

1. O. Kahn, ed.: A.G. Sykes, In Advances in Inorganic Chemistry, vol. 43, Academic Press; San Diego, p. 179 (1995).
2. K.S. Murray, In Advances in Inorganic Chemistry, Vol. 43, A.G. Sykes, Ed.; Academic Press; San Diego, p. 261 (1995).
3. D.M. Rudkevich, J.D. Mercer-Chalmers, W. Verboom, R. Ungaro, F. de Jong and D.N. Reinhoudt, *J. Am. Chem. Soc.*, **117**, 6124 (1995); https://doi.org/10.1021/ja00127a027
4. D.M. Rudkevich, W. Verboom, Z. Brzozka, W.P.R.V. Stauthamer, M.J. Palys, G.J. van Hummel, S.M. Franken, S. Harkema, J.F.J. Engbersen and D.N. Reinhoudt, *J. Am. Chem. Soc.*, **116**, 4341 (1994); https://doi.org/10.1021/ja00089a023
5. P.A. Vigato, S. Tamburini and D.E. Fenton, *Coord. Chem. Rev.*, **106**, 25 (1990); https://doi.org/10.1016/0010-8545(60)80002-1
6. J.A. Tainer, E.D. Getzoff, K.M. Beem, J.S. Richardson and D.C. Richardson, *J. Mol. Biol.*, **160**, 181 (1982); https://doi.org/10.1016/0022-2836(82)90174-7
7. J.A. Tainer, E.D. Getzoff, J.S. Richardson and D.C. Richardson, *Nature*, **306**, 284 (1983); https://doi.org/10.1038/306284a0
8. N. Sträter, T. Klabunde, P. Tucker, H. Witzel and B. Krebs, *Science*, **268**, 1489 (1995); https://doi.org/10.1126/science.7770774
9. C.R. Kissinger, H.E. Parge, D.R. Knighton, C.T. Lewis, L.A. Pelletier, A. Tempczyk, V.J. Kalish, K.D. Tucker, R.E. Showalter, E.W. Moomaw, L.N. Gastinel, N. Habuka, X. Chen, F. Maldonado, J.E. Barker, R. Bacquet and J.E. Villafranca, *Nature*, **378**, 641 (1995); https://doi.org/10.1038/378641a0
10. I. Bertini, L. Banci and C. Luchinat, ed.: L. Que, Jr., Metal Clusters in Proteins; ACS Symposium Series 372; American Chemical Society: Washington, DC, pp. 71-84 (1988).
11. L. Que Jr. and A.E. True, *Prog. Inorg. Chem.*, **38**, 97 (1990); https://doi.org/10.1002/9780470166390.ch3
12. J.B. Vincent, G.L. Olivier-Lilley and B.A. Averill, *Chem. Rev.*, **90**, 1447 (1990); https://doi.org/10.1021/cr00106a004
13. A.L. Feig and S.J. Lippard, *Chem. Rev.*, **94**, 759 (1994); https://doi.org/10.1021/cr00027a011
14. K.A. Magnus, H. Ton-That and J.E. Carpenter, *Chem. Rev.*, **94**, 727 (1994); https://doi.org/10.1021/cr00027a009
15. E.I. Solomon, M.J. Baldwin and M.D. Lowery, *Chem. Rev.*, **92**, 521 (1992); https://doi.org/10.1021/cr00012a003
16. W.H. Lang and K.E. van Holde, *Proc. Natl. Acad. Sci. USA*, **88**, 244 (1991); https://doi.org/10.1073/pnas.88.1.244
17. D.E. Fenton and H. Ôkawa, *Chem. Ber.*, **130**, 433 (1997); https://doi.org/10.1002/cber.19971300402
18. H. Ôkawa, H. Furutachi and D.E. Fenton, *Coord. Chem. Rev.*, **174**, 51 (1998); https://doi.org/10.1016/S0010-8545(97)00082-9
19. D.E. Fenton, In Advances in Inorganic and Bioinorganic Mechanism, Vol. 43, A.G. Sykes, Ed.; Academic Press; London, p. 187 (1983).
20. H. Furutachi and H. Ôkawa, *Inorg. Chem.*, **36**, 3911 (1997); https://doi.org/10.1021/ic9700563
21. J.D. Crane, D.E. Fenton, J.M. Latour and A.J. Smith, *J. Chem. Soc., Dalton Trans.*, 2979 (1991); https://doi.org/10.1039/dt9910002979
22. C. Fraser, L. Johnston, A.L. Rheingold, B.S. Haggerty, G.K. Williams, J. Whelan and B. Bosnich, *Inorg. Chem.*, **31**, 1835 (1992); https://doi.org/10.1021/ic00036a022
23. D.G. McCollum, G.P.A. Yap, A.L. Rheingold and B. Bosnich, *J. Am. Chem. Soc.*, **118**, 1365 (1996); https://doi.org/10.1021/ja952873c
24. P. Kamaras, M.C. Cajulis, M. Rapta, G.A. Brewer and G.B. Jameson, *J. Am. Chem. Soc.*, **116**, 10334 (1994); https://doi.org/10.1021/ja00101a077
25. Y. Hayashi, T. Kayatani, H. Sugimoto, M. Suzuki, K. Inomata, A. Uehara, Y. Mizutani, T. Kitagawa and Y. Maeda, *J. Am. Chem. Soc.*, **117**, 11220 (1995); https://doi.org/10.1021/ja00150a020
26. J.H. Satcher Jr., M.W. Droege, T.J.R. Weakley and R.T. Taylor, *Inorg. Chem.*, **34**, 3317 (1995); https://doi.org/10.1021/ic00116a026
27. B. Eulering, M. Schmidt, U. Pinkernell, U. Karst and B. Krebs, *Angew. Chem. Int. Ed. Engl.*, **35**, 1973 (1996); https://doi.org/10.1002/anie.199619731
28. D. Volkmer, A. Hörstmann, K. Griesar, W. Haase and B. Krebs, *Inorg. Chem.*, **35**, 1132 (1996); https://doi.org/10.1021/ic950368a
29. D. Volkmer, B. Hommerich, K. Griesar, W. Haase and B. Krebs, *Inorg. Chem.*, **35**, 3792 (1996); https://doi.org/10.1021/ic951567x
30. M. Konrad, F. Meyer, K. Heinze and L. Zsolnai, *J. Chem. Soc., Dalton Trans.*, 199 (1998); https://doi.org/10.1039/a705543i
31. M. Konrad, S. Wuthe, F. Meyer and E. Kaifer, *Eur. J. Inorg. Chem.*, 2233 (2001); https://doi.org/10.1002/1099-0682(200109)2001:9<2233::AID-EJIC2233>3.0.CO;2-4

32. Q.Y. Chen, Q.-H. Luo, Z.-L. Wang and J.-T. Chen, *Chem. Commun.*, 1033 (2000); https://doi.org/10.1039/a909926n
33. H. He, A.E. Martell, R.J. Motekaitis and J.H. Reibenspies, *Inorg. Chem.*, **39**, 1586 (2000); https://doi.org/10.1021/ic9911264
34. N.C. Gianneschi, C.A. Mirkin, L.N. Zakharov and A.L. Rheingold, *Inorg. Chem.*, **41**, 5326 (2002); https://doi.org/10.1021/ic025875o
35. M. Botta, U. Casellato, C. Scalco, S. Tamburini, P. Tomasin, P.A. Vigato, S. Aime and A. Barge, *Chem. Eur. J.*, **8**, 3917 (2002); https://doi.org/10.1002/1521-3765(20020902)8:17<3917::AID-CHEM3917>3.0.CO;2-D
36. S. Bhattacharyya, D. Ghosh, S. Mukhopadhyay, W.P. Jensen, E.R.T. Tiekink and M. Chaudhury, *J. Chem. Soc., Dalton Trans.*, 4677 (2000); https://doi.org/10.1039/b005906o
37. D.D. Perrin, W.L.F. Armarego and D.R. Perrin, Purification of Laboratory Chemicals, Pergamon: Oxford, England, edn. 2 (1980).
38. W.R. Robinson, *J. Chem. Educ.*, **62**, 1001 (1985); https://doi.org/10.1021/ed062p1001
39. N. Walker and D. Stuart, *Acta Crystallogr. A*, **39**, 158 (1983); https://doi.org/10.1107/S0108767383000252
40. SADABS, v 2.01, Bruker AXS Inc., Madison, WI, USA (2000).
41. P.T. Beurskens, G. Admiraal, G. Beurskens, W.P. Bosman, S. García-Granda, J.M.M. Smits and C. Smykalla, The DIRDIF Program System, Technical Report of the Crystallography Laboratory, University of Nijmegen, Netherlands (1992).
42. G.M. Sheldrick, SHELXL-97, Program for Crystal Structure Refinement; University of Göttingen: Göttingen, Germany (1997).
43. C.K. Johnson, 'ORTEP II', Report ORNL-5138; Oak Ridge National Laboratory, TN, USA (1976).
44. teXsan: Structure Analysis Software; Molecular Structure Corporation: The Woodlands, TX, USA (1997).
45. K. Abe, K. Matsufuji, M. Ohba and H. Ôkawa, *Inorg. Chem.*, **41**, 4461 (2002); https://doi.org/10.1021/ic020002f
46. H. Adams, D.E. Fenton, S.R. Haque, S.L. Heath, M. Ohba, H. Ôkawa and S.E. Spey, *J. Chem. Soc., Dalton Trans.*, 1849 (2000); https://doi.org/10.1039/b0013951
47. C. Juarez-Garcia, M.P. Hendrich, T.R. Holman, L. Que Jr. and E. Münck, *J. Am. Chem. Soc.*, **113**, 518 (1991); https://doi.org/10.1021/ja00002a020
48. T.R. Holman, C. Juarez-Garcia, M.P. Hendrich, L. Que Jr. and E. Münck, *J. Am. Chem. Soc.*, **112**, 7611 (1990); https://doi.org/10.1021/ja00177a024
49. A.S. Borovik, V. Papaefthymiou, L.F. Taylor, O.P. Anderson and L. Que Jr., *J. Am. Chem. Soc.*, **111**, 6183 (1989); https://doi.org/10.1021/ja00198a032
50. M. Suzuki, S. Fujinami, T. Hibino, H. Hori, Y. Maeda, A. Uehara and M. Suzuki, *Inorg. Chim. Acta*, **283**, 124 (1998); https://doi.org/10.1016/S0020-1693(98)00226-6
51. G. Murphy, P. Nagle, B. Murphy and B. Hathaway, *J. Chem. Soc., Dalton Trans.*, 2645 (1997); https://doi.org/10.1039/a702291c
52. G. Murphy, C. O'Sullivan, B. Murphy and B. Hathaway, *Inorg. Chem.*, **37**, 240 (1998); https://doi.org/10.1021/ic970458a
53. A.W. Addison, T.N. Rao, J. Reedijk, J. van Rijn and G.C. Verschoor, *J. Chem. Soc., Dalton Trans.*, 1349 (1984); https://doi.org/10.1039/DT9840001349
54. S. Bhattacharyya, S.B. Kumar, S.K. Dutta, E.R.T. Tiekink and M. Chaudhury, *Inorg. Chem.*, **35**, 1967 (1996); https://doi.org/10.1021/ic950594k
55. S.B. Kumar, S. Bhattacharyya, S.K. Dutta, E.R.T. Tiekink and M. Chaudhury, *J. Chem. Soc., Dalton Trans.*, 2619 (1995); https://doi.org/10.1039/dt9950002619
56. D. Ghosh, N. Kundu, G. Maity, K.-Y. Choi, A. Caneschi, A. Endo and M. Chaudhury, *Inorg. Chem.*, **43**, 6015 (2004); https://doi.org/10.1021/ic049449+
57. B.J. Hathaway and D.E. Billing, *Coord. Chem. Rev.*, **5**, 143 (1970); https://doi.org/10.1016/S0010-8545(00)80135-6
58. A.B.P. Lever, Inorganic Electronic Spectroscopy, Elsevier: New York, edn 2 (1984).
59. M. Ciampolini, *Struct. Bonding (Berlin)*, **6**, 52 (1969); https://doi.org/10.1007/BFb0118854
60. J.S. Wood, *Inorg. Chem.*, **7**, 852 (1968); https://doi.org/10.1021/ic50063a002
61. J.L. Hughey IV, T.G. Fawcett, S.M. Rudich, R.A. Lalancette, J.A. Potenza and H.J. Schugar, *J. Am. Chem. Soc.*, **101**, 2617 (1979); https://doi.org/10.1021/ja00504a020
62. M. Yonemura, Y. Matsumura, H. Furutachi, M. Ohba, H. Ôkawa and D.E. Fenton, *Inorg. Chem.*, **36**, 2711 (1997); https://doi.org/10.1021/ic9614430